Analyst

Cite this: *Analyst*, 2012, **137**, 5538

www.rsc.org/analyst

PAPER

Ultrasensitive on-column laser-induced fluorescence in capillary electrophoresis using multiparameter confocal detection†

Amir Mazouchi,[a] Bryan J. Dodgson,[b] David W. Wegman,[b] Sergey N. Krylov*[b] and Claudiu C. Gradinaru*[a]

Received 25th July 2012, Accepted 3rd October 2012
DOI: 10.1039/c2an36016k

We report a simple method to efficiently couple on-column, standard Capillary Electrophoresis with Confocal MultiParameter Fluorescence detection (CE-CMPF) using only commercially available components. A molecular collection of 13% and a concentration limit of detection of 1.5 pM fluorescein are achieved in our instrument by gating the arrival time of individual photons in order to reduce the scattering contribution. The proposed scheme allows for amplification-free detection and separation of three different microRNAs from the MCF-7 cell lysate. The limit of detection is approximately 500 times smaller and the separation time is 3 times shorter compared to protocols based on commercial CE instrumentation. Although the optical design can be further improved, it is shown that the current CE-CMPF prototype is already capable of analyzing the microRNA content of single cells. In addition, all CE protocols previously developed for commercial instruments can be performed with our CE-CMPF without modification but with nearly 3 orders of magnitude better limit of detection.

1. Introduction

Capillary Electrophoresis with Laser-Induced Fluorescence (CE-LIF) detection is a highly versatile analytical tool. Using commercially available CE-LIF instruments, protocols have been developed for applications ranging from DNA sequencing[1–3] to kinetic rate constant measurements[4–6] and from affinity analysis[7–9] to analysis of enantiomers,[10,11] *etc.* With such a wide range of uses, these instruments are beneficial for various pharmaceutical, genetic, and biomedical investigations. In addition to their versatility, commercial CE-LIF instruments are also easy-to-use as they provide for fully automated injection, separation, and collection of samples and on-column fluorescence detection through the capillary wall. Therefore, the majority of practical CE protocols have been developed for commercially available instruments.

While on-column detection allows for easy alignment, it also comes with an increase of the background signal due to Rayleigh and Raman scattering as well as capillary autofluorescence.[12] This affects the signal-to-noise ratio (*S*/*N*) and restricts the detection limit of these instruments to the order of 10^4 to 10^5 injected fluorophore molecules. Furthermore, it reduces the available dynamic range of CE-LIF methods.

In discussing the sensitivity of fluorescence detection for CE-LIF we first define some necessary terms: the mass Limit of Detection (mLOD) is the minimum number of molecules (not necessarily all pass through the detection volume) in a plug such that the plug is detectable; the Molecular Counting Efficiency (MCE) is the fraction of injected molecules that pass through the laser probe volume; the absolute Limit of Detection (LOD) is the minimum number of molecules required to pass through the laser probe volume such that the plug is detectable (approximately equal to MCE × mLOD); and the concentration LOD (cLOD) is the minimum concentration of a plug such that it is detectable. For all the terms mentioned above the phrase "such that is detectable" refers to a CE peak with a $S/N = 3$. The first CE-LIF approach that was developed to address fluorescence sensitivity employed post-column detection using a sophisticated sheath-flow cuvette to detect analytes after they exited the capillary.[12,13] This technique was adopted from flow cytometry and reduces the background signal by eliminating scattering and auto-fluorescence originating from the capillary walls. Using this design mLODs of less than 100 molecules were reported nearly 20 years ago.[14,15] More recently, this design was used to achieve 9-orders of magnitude dynamic range for fluorescent detection[16] (pM–mM concentrations). Despite the effectiveness of this technique, there are no current commercial implementations of this approach, probably because inherent difficulties with sample collection, capillary exchange and alignment procedures.

Another approach proposed for sensitive CE-LIF was the use of (sub)micrometer-sized separation channels. Such designs force all analytes to flow through a tightly focused excitation beam, thus improving the MCE. Examples of micro-channel designs include custom-made pinched capillaries,[17] microfluidic

[a]*Department of Physics, University of Toronto and Department of Chemical and Physical Sciences, University of Toronto Mississauga, Mississauga, Ontario L5L 1C6, Canada. E-mail: claudiu.gradinaru@utoronto.ca*
[b]*Department of Chemistry and Centre for Research on Biomolecular Interactions, York University, Toronto, Ontario M3J 1P3, Canada. E-mail: skrylov@yorku.ca*
† Electronic supplementary information (ESI) available. See DOI: 10.1039/c2an36016k

chips,[18–21] etched glass channels,[22] patch-clamp pipettes,[23,24] and quartz capillaries.[23] The use of micro-channels often hinders diffusion in 1 or 2 dimensions, thus beneficially causing molecules to reside in the detection volume longer and emit more photons.[23,24] Single molecule fluorescence bursts with $S/N \approx 50$ were recorded;[18] however, the drawback of the method is that small-size channels are more prone to contamination and clogging.[19,25,26] Consequently, there is only one micro-channel study involving a complex biological sample (cell lysate) which avoids the aforementioned troubles by using a relatively wide channel (1.8 μm × 60 μm).[19] In addition, the shape and material of micro-channels often differ from that of standard fused silica capillaries. This difference may introduce changes to analyte migration speeds and retention times,[17,23] analyte velocity profiles,[19,27] and electro-osmotic flows from those determined in a standard round capillary. The variations in these parameters can make transferring protocols from commercial instruments to micro-channel devices non-trivial. Also, the medium that electrophoresis is being carried out in is known to degrade over time and must be replaced; further making the case for the use of inexpensive and easy-to-replace commercial round capillaries rather than more complicated chips and custom-made capillaries.

Therefore, present CE-LIF designs that offer improved fluorescence limits of detection over commercial instruments also reduce the compatibility of these designs with the pre-existing protocols. Furthermore, many designs use custom-made components that can only be reproduced with access to specialized expertise and/or facilities. To date there is no a highly sensitive CE-LIF design that would use the same schematic as commercial CE instruments, namely on-column detection using a standard fused silica capillary. In this report, we propose a method to efficiently couple on-column, standard Capillary Electrophoresis with Confocal and MultiParameter Fluorescence detection (CE-CMPF) using only commercially available components. The resulting design can perform any protocol previously developed on a commercial device, but with an improvement of the limit of detection of nearly 3 orders of magnitude. Additionally, by avoiding the use of custom-made components, our design can be easily implemented in other research labs.

The performance of the instrument was tested through a standard limit of detection experiment using a fluorescein dye. Through optimizing the parameters of the detector, we achieved an LOD of 5 molecules of fluorescein. To confirm that our setup could perform protocols developed on a commercial instrument we then carried out a pre-existing protocol, direct quantitative analysis of multiple miRNAs (DQAMmiR), for the amplification/modification-free detection of miRNA from cell lysate.[28] Not only are the results achieved using a commercial instrument replicated, but baseline separation is carried out in one-third of the time and the mLOD is enhanced 500 times. Furthermore, the analysis of samples of cellular lysate was demonstrated with no loss of generality with respect to the studies done using commercial CE-LIF instruments. We conclude our analysis by showing that our instrument is capable of analyzing the amount of lysate from a single cell, thus indicating that our design could potentially have widespread applications for single-cell analysis[29] and cancer diagnostics by fine-needle aspiration biopsy.

2. Materials and methods

2.1. Capillary electrophoresis

To construct the embedded capillary interface (ECI), we first created a 2 cm detection window in the capillary (TSP010150, Polymicro Tech., Phoenix, AZ, USA) by removing the capillary's polyimide coating under an open flame for several seconds. The detection window and the surface of the microscope coverslip (Gold Seal #3223, Electron Microscopy Sciences, Hatfield, PA, USA) were cleaned using ethanol and the detection window was then carefully pressed onto the coverslip using the plastic prongs of tweezers, which were held roughly 1 cm apart. A small bead of adhesive (NOA61, Thorlabs, Newton, NJ, USA) was placed directly in between the two prongs and the bead was cured under a UV lamp for 1 min. The prongs were then removed and the rest of the bare capillary resting on the coverslip was coated in adhesive (to reduce fragility) and cured for 2–3 min.

Fluorescence detection was performed by placing the ECI device on top of a multiparameter confocal microscope described in the following section. Samples were injected into the capillary by negatively pressurizing an airtight chamber sealed to the outlet end of the capillary. The chamber was pressurized by drawing back the plunger on a 60 mL syringe by a pre-defined distance for a pre-defined duration of time. The exact distance and duration were controlled using an automated syringe pump (NE-1010, New Era Pump Systems Inc., Farmingdale, NY, USA). The total amount of sample injected was determined by experimentally measuring the flow rate of a fluorescent dye under the pre-defined injection pressure then using this flow rate to determine injection volumes for fixed injection durations. 200 pL injections were performed by beginning with the syringe plunger at the 0 mL mark, drawing the plunger back to the 5 mL mark, holding for 5 s, then returning the plunger to the 0 mL mark and opening the chamber to the atmosphere. 60 and 30 pL injections were performed by beginning with the syringe plunger at the 10 mL mark, then drawing the plunger back to the 12 mL mark, holding for 10 and 5 s, respectively, then returning the plunger back to the 10 mL mark and opening the chamber to the atmosphere. Electrophoresis was carried out by placing a platinum electrode in the inlet and outlet vials and using a high voltage power supply (CZE1000r Spellman, Hauppauge, NY, USA) to provide an electric field of 300 V cm^{-1} across the capillary's length. The running buffer was 25 mM sodium tetraborate, pH 9.3, with 50 nM single-stranded DNA binding protein (SSB) from *E. coli* (SSB02200, Epicentre Biotechnologies, Madison, WI, USA) added to the buffer for miRNA detection experiments. The capillary was flushed prior to every CE run with 0.1 M HCl, 0.1 M NaOH, deionized H_2O, and running buffer for 1 min each. The total length of the capillary was ~50 cm and the length from the injection end to the detection point was ~7 cm.

2.2. CE-CMPF instrument

Time- and polarization-resolved laser-induced fluorescence measurements were performed on a multiparameter confocal microscope described in detail elsewhere.[30,31] A Ti:sapphire laser (Tsunami HP, Spectra Physics, Santa Clara, CA, USA) was used as the excitation source, producing laser pulses of ~100 fs

duration and 10–12 nm spectral width. The output was tuned to a center wavelength of 956 nm and frequency doubled to 478 nm by focusing the laser beam onto a β-BBO crystal. A dichroic mirror directed laser light to a 1.4 NA/100× oil immersion microscope objective (PlanApochromat, Carl Zeiss, Toronto, Canada). The embedded capillary interface (ECI) was mounted on a three-axis piezo scanner (T225, MadCity Labs, Madison, WI, USA), which controls the position and depth of the focus onto the capillary.

The fluorescence was collected by the same objective and the excitation laser scattering was removed by a series of long-pass and band-pass spectral filters. Light was passed through a 150 μm pinhole for confocal detection and then it was directed either fully to a single-photon avalanche diode (SPAD) detector (PD5CTC, Optoelectronic Components, Kirkland, Canada) or split by a broadband polarizer cube into components and focused onto two SPADs.

Measurements were performed in the Time-Tagged Time-resolved (T3) mode. In this mode, the output of the SPAD and a small fraction of the laser excitation pulse, as detected by a fast photodiode (PHD-400-N, Becker & Hickl, Berlin, Germany), were used as inputs for the Time-Correlated Single-Photon Counting (TCSPC) module (PicoHarp300, PicoQuant, Berlin, Germany). The delay between the excitation pulse and the detected photon (start–stop time), and the absolute arrival time of each photon are recorded with 4 ps resolution and up to a maximum count rate of 10 MHz. Custom LabView codes were developed to control photon data acquisition, process the data and visualize intensity time-trajectories and start–stop (lifetime) histograms.

2.3. Commercial CE instrument

We used a P/ACE MDQ capillary electrophoresis system (Beckman-Coulter, Fullerton, CA, USA) with laser-induced fluorescence detection. Fluorescence was excited with a 488 nm continuous wave solid-state laser (JDSU, Santa Rosa, CA, USA). We used bare fused-silica capillaries with an outer diameter of 365 μm, an inner diameter of 75 μm, and a total length of 50 cm. The distance from the injection end of the capillary to the detector was 39 cm. The running buffer was 25 mM sodium tetraborate, pH 9.3, with 50 nM SSB. The capillary was flushed prior to every CE run with 0.1 M HCl, 0.1 M NaOH, deionized H_2O, and running buffer for 1 min each. Samples were injected by a pressure pulse of 0.5 psi for 5 s, the volume of the injected sample was ~6 nL. Electrophoresis was driven by an electric field of 500 V cm^{-1}. Electropherograms were analyzed using 32Karat Software. Peak areas were divided by the corresponding migration times to compensate for the dependence of the residence time in the detector on the electrophoretic velocity of species. For electropherograms from both instruments all areas were normalized by dividing them by the area of internal standard, fluorescein.

2.4. Sample preparation

To calibrate the optical system, 200 nm fluorescent micro-spheres (F8809, Invitrogen, Grand Island, NY, USA) were chemically immobilized onto the surface of the inner bore of the capillary. Polyethyleneimide was injected and incubated in the capillary, followed by rinsing with water, then the injection and incubation of a solution of fluorescent micro-spheres, followed by another rinsing step with water and finally drying by flowing air (14 psi) through it. The duration of each step was 5 minutes.

Two fluorescent dyes, Rhodamine110 (Rh110) (20310, Biotium Inc., Hayward, CA, USA) and fluorescein (F6377, Sigma Aldrich, Oakville, ON, Canada), were prepared in a buffer of 50 mM Tris–acetate, 50 mM NaCl, 10 mM EDTA, pH 7.8. The limit of detection of the CE-CMPF instrument was determined by analyzing the signal from injections of fluorescein. Separate samples of 100, 50, 25, 12.5, and 6 pM fluorescein were injected into a capillary pre-filled with 25 mM sodium tetraborate (pH 9.3). The fluorescein samples were injected by sealing the outlet vial to the syringe and programming the syringe pump to draw the syringe back, hold for 10 s, and then return to its initial position. The volume of sample injected was determined by finding the propagation speed of fluorescein under the pressure of the syringe with no voltage applied. By drawing the syringe back to the 2 mL mark, with an initial dead volume of 10 mL, the speed of propagation was measured to be 0.09 mm s^{-1}, and the pressure of injection was determined to be approximately 2.4 psi using the Hagen–Poiseuille equation. Under these conditions, 70 pL of sample was injected in 10 s.

The CE-based DQAMmiR method was applied for detection of different micro(mi)RNA species (mir21, mir145 and mir145 synthesized by IDT, Coralville, IA, USA) using a procedure described previously.[28] Briefly, the miRNAs were hybridized to single-stranded (ss) DNA probes labelled with Alexa-488 in the incubation buffer (50 mM Tris–acetate, 50 mM NaCl, 10 mM EDTA, pH 7.8). Each miRNA species was diluted to a concentration of 100 pM for CE-CMPF-ECI or 2 nM for commercial CE, with a 5-fold excess of probe ssDNA in each case, while the samples of MCF-7 cell lysate were used at 2.72×10^7 cells per mL and 118×10^7 cells per mL, respectively. Also included in the mixtures for commercial CE were 10 nM fluorescein, 5 μM masking DNA (20-nucleotide DNA strand and 2 μM masking RNA (tRNA library), while for CE-CMPF-ECI they were all reduced by a factor of 20. The fluorescein was added as an internal standard to help quantify variations in the volume of injected sample and in peak migration times. The masking DNA and RNA were added to prevent the degradation of DNA and RNA, respectively, as well as to prevent adsorption of the probe or the miRNA to the walls of the vial during incubation. Sample injection volumes were 6 nL for the commercial CE instrument, 200 pL for CE-CMPF-ECI instrument, and 30 pL for the injection of the equivalent lysate of a single cell using CE-CMPF-ECI.

Pre-existing DNA or RNA structures were denatured by raising the temperature of the mixture to 80 °C, and hybridization was promoted by cooling the mixture to 37 °C at a rate of 20 °C min^{-1}. The mixture was incubated at 37 °C overnight to ensure complete hybridization without optimizing the hybridization time. To determine the miRNA detection limit, a single DNA probe–miRNA pair was used and SSB was removed from the run buffer. The uncertainty on the limit of detection of microRNA was ±20% (one standard deviation) as determined by measuring the run-to-run variations in peak area from 30 pL injections of the various concentrations of microRNA, which

were performed in triplicate and normalized by the area of the fluorescein internal standard.

Cell lysates were prepared in the following way: MCF-7 cells were purchased from ATCC and grown in incubator at 37 °C in the atmosphere of 5% CO_2. Cells were grown in DMEM/F12 medium (Invitrogen, Carlsbad, CA, USA) with 20 ng mL^{-1} hEGF, 0.5 μg mL^{-1} hydrocortisone, 10 μg mL^{-1} insulin, FBS and 10 000 μg mL^{-1} penicillin, streptomycin in a 100 mm Petri dish. When cells covered roughly 90% of the plate they were washed with PBS, trypsinized to be detached from the bottom of dish and centrifuged at 150 × *g* for 5 min. Pellet was washed twice with PBS. The cells were counted using a haemocytometer and lysed with 1% Triton in 50 mM Tris–acetate, 50 mM KCl, 10 μM masking RNA, 0.1 mM EDTA, pH 8.16. Cell lysates were aliquoted and stored in liquid nitrogen for further use.

3. Results and discussion

In order to improve the detection limit, the problem of high background due to, *i.e.*, (i) the reflections of excitation beam at the capillary walls, (ii) the Raman scattering of water, and (iii) the autofluorescence of the capillary glass, must be addressed without altering the on-column detection scheme. To this end, we implemented detection techniques and data analysis used in single-molecule fluorescence spectroscopy. Axial resolution in the direction of beam propagation is achievable with a confocal detection scheme, which suppresses out-of-focus background photons originating from Rayleigh and Raman scattering and from fluorescence impurities. This technique can, therefore, be used to address points (i) and (iii) by limiting the axial size of the focal volume to within the inner bore of the capillary, and point (ii) through limiting the amount of buffer that is optically sampled. Under typical experimental conditions a well-designed confocal microscope allows for highly sensitive fluorescence detection with single molecule resolution in a detection volume less than 1 fL. Our goal in this work was to effectively couple ultrasensitive confocal fluorescence detection with a standard commercial round capillary.

3.1. CE integration on a confocal microscope

To efficiently couple the confocal detection system with the CE-LIF platform we had to avoid the pitfalls of previous confocal-CE studies: poor MCE (<0.1%) in capillaries much larger than the size of the detection volume[32,33] and clogging in sub-micrometer channels.[19] With these studies in mind, we chose to use a capillary with a 10 μm inner diameter (ID) and a standard confocal detection volume. For this ID value, commercially available capillaries have outer diameters (OD) greater than 150 μm resulting in an OD/ID > 15. At such large ratios distortions of the detection volume by lensing effects and spherical aberrations due to the curvature and wall thickness of capillaries can be so severe that even bright samples like 20 nm fluorescent beads may pass undetected in a confocal-CE arrangement.[17] Therefore, careful choice of capillary geometry and mounting medium is essential to limit the distortion of the detection volume.

The microscope objective used in this study (Zeiss PlanApochromat, 1.4 NA oil) is compensated against spherical aberrations when used with 170 μm thick coverslips. It is very sensitive to deviations from this thickness and, therefore, the interface between the objective and the capillary inner bore was designed to be close to 170 μm and to have a uniform refractive index near that of glass. To achieve these requirements we proposed the use of an ECI, whereby the capillary was fixed to a support surface by means of a transparent matrix (Fig. 1, left). The thickness of the support surface had to be less than 170 μm so we chose to use a commercially available 110 μm coverslip. The use of a commercially available capillary with an inner diameter of 10 μm, an outer diameter of 150 μm and wall thickness of 58 μm (after the opaque 12 μm polyimide coating was removed under a flame) ensured a final thickness of 168 μm, thus mimicking a standard coverslip. The 2 μm deviation between the ECI and the optimum coverslip thickness, although not negligible, is within the 3 μm uncertainty in capillary thickness provided by the manufacturer and the <5 μm measured uncertainty of our coverslip batch. For the purposes of this study this deviation should be acceptable.

The capillary and support surface were fixed together using an optical transparent adhesive with a refractive index of 1.56. By closely matching the refractive index of fused silica (1.46), borosilicate glass (1.52), and immersion oil (1.53) the extent of scattering and aberrations is reduced (Fig. 1, right). In addition, back-scattering was further reduced by mounting the ECI along the *y*-axis parallel to the laser polarization.[34] The capillary was aligned on the 3-D piezo stage by maximizing the back-scattering signal from the glass–air interface (see ESI†). Once the capillary inner bore was located, a sample of 100 nM Rhodamine 110 was passed through the capillary. Fig. 2 depicts the back-scattering and the fluorescence signals as a function of focal point distance, as measured from the wall of the inner bore closest to the objective. The fluorescence intensity has a maximum at ~4.5 μm from the wall, which closely corresponds to the optimum depth found previously (5 μm) to produce minimum aberration when using this oil objective for aqueous measurements on a regular coverslip.[31] All subsequent CE measurements were made with the stage translated 4.5 μm into the capillary.

3.2. The detection volume in the capillary

In order to estimate the aberrations introduced by the ECI we immobilized fluorescent polystyrene beads on the inner wall of

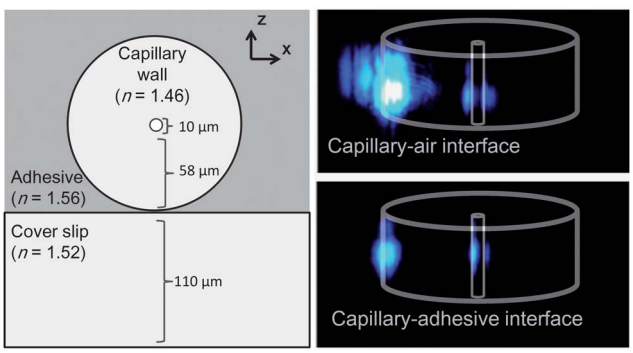

Fig. 1 Left: schematic diagram showing geometry and refractive indices of ECI. Right: photographs demonstrating the result of a laser beam incident on a 10 μm inner diameter capillary in air, and one embedded in a transparent matrix of adhesive (the sketch of the capillary is a guide to the eye).

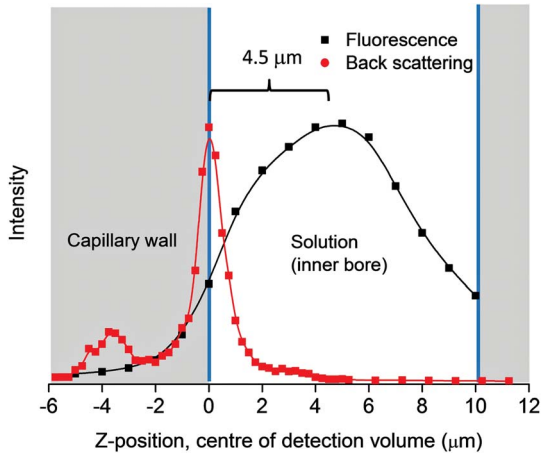

Fig. 2 Backscattering from a dry capillary (red circles) and fluorescence intensity measured in relative units from a capillary filled with a sample of 100 nM Rhodamine 110 (black squares) as functions of distance from the inner bore wall. Signal maximum for fluorescence roughly corresponds to centre of inner bore.

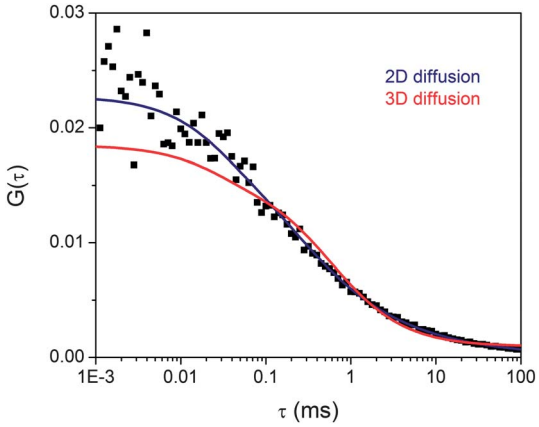

Fig. 3 Experimental FCS curve of 10 nM Rhodamine 110 measured on the ECI platform (black squares) fitted by 2D and 3D diffusion models.

the capillary and imaged them on the confocal microscope. A series of images taken at different axial (z) positions showed two transverse focal points separated by ~4 μm along the z-axis (see ESI†). At each of the focal points the bead image was elongated nearly 4–6 times in the other direction. This astigmatism is likely caused by the cylindrical lensing effect of the curved capillary wall. Upon filling the capillary with deionized water, the astigmatism decreased considerably such that the two separate focal points were no longer distinguishable. The bead image assumes the same symmetrical shape as when immobilized to a standard coverslip; however, the image of the ECI-immobilized bead is ~1.5 times larger, in both directions (see ESI†).

We also compared the fluorescence intensity from a dye sample (100 nM Rh110), as measured in the ECI and on a standard coverslip. Under similar conditions, the signal from the ECI sample was found to be one-third of that from the coverslip sample. Since Rh110 is known not to adsorb to either borosilicate coverslips,[31] fused silica capillaries or sample vials,[35] the fluorescence reduction in ECI should be entirely ascribed to optical aberrations. These can manifest as lower excitation intensity caused by focal spot expansion (illustrated by bead imaging) and a lower photon-collection efficiency. To determine the individual contribution of beam expansion and collection efficiency to the overall 3-fold fluorescence reduction we first needed to estimate the size of the detection volume in the ECI. This was addressed by Fluorescence Correlation Spectroscopy (FCS) analysis (see ESI†). FCS provides geometrical parameters of the 3-D detection volume inside the capillary. The correlation curve for freely diffusing Rhodamine dye in the capillary fits perfectly to the 2-D (and badly to the 3-D) diffusion model (Fig. 3), implying that the detection volume extends across almost the entire inner capillary bore. The FCS fit yields a lateral radius of the confocal volume of 0.43 μm, suggesting a ~1.3× lateral expansion of the ECI detection volume. The disagreement between this number and beam expansion measured by bead imaging (1.5 times) is probably due to the fact that bead imaging took place on the curved surface of the inner bore, whereas the FCS measurement was taken 4.5 μm into solution. The expanded axial and transverse radii suggested an overall ~3.3× expansion in total detection volume compared to the same experiment performed on a coverslip.

The relative reduction in collection efficiency, as compared to a measurement made on a coverslip, can be estimated from a simple relation $F \propto NIC_{ph}$, where F is the measured fluorescence intensity, N is the average number of molecules in the detection volume, I is the beam intensity at the focal spot, and C_{ph} is the photon collection efficiency. Experimentally, we found that F was reduced by a factor of 3, N, which is proportional to the size of the detection volume, increased by a factor of ~3.3, and I decreased by a factor of ~1.7(1.3 × 1.3). By implementing these values in the expression above, we found that C_{ph} for the ECI mode was about 5-fold lower than the typical value for the coverslip mode, *e.g.*, 2.7%.[31] In future iterations of the design, the photon collection efficiency can be improved by choosing SPAD detectors with larger photoactive area and with higher quantum efficiency and by employing corrective lenses that minimize the optical aberrations.

3.3. *S*/*N* optimization

While the preceding discussion identified the theoretical limit to ECI-based measurements as set by the optics of the system, in the next section, we seek improvements to the detection limit through optimizing the *S*/*N* ratio using different experimental conditions and data analysis techniques. To calculate the *S*/*N* ratio, the signal was found by subtracting the baseline from the peak amplitude and the noise is considered to be the standard deviation of the baseline.

3.3.1. Time binning. The advantage of time-tagged photon detection is that the fluorescence signal can be binned post-acquisition at any desired dwell time. To explore the influence of data binning on *S*/*N*, we performed electrophoresis of a 60 pL of sample containing 100 pM fluorescein, 5 nM Alexa-488 labelled DNA, and 100 pM unlabelled complementary strand of RNA (Fig. 4). A maximum *S*/*N* for fluorescein was obtained using a bin size of 800 ms, while the maximum *S*/*N* for the duplex peak occurred when we chose a 400 ms bin. The smaller bin size for

maximum *S*/*N* in the latter case was presumably due to the fact that the duplex peak is narrower than that of fluorescein. To ensure that the *S*/*N* is close to optimal for both simple fluorescent dyes as well as for biomolecular complexes, we chose a compromise value of 600 ms for the time bin in all subsequent measurements.

3.3.2. Excitation power. Long plugs of 100 pM fluorescein (peak width of more than 10 s) were injected into the capillary by negative pressure to study the effect of the excitation power on the *S*/*N* ratio. The excitation power was optimized by varying the laser power and measuring the resulting *S*/*N* from the sample. An optimum value of 200 μW was determined which gave an estimated focal plane intensity of 35 kW cm^2 based on the FCS-measured focal point radius of 0.43 μm. This optimum power was used for all subsequent measurements.

3.3.3. Polarization and lifetime filtering. By placing a polarizer cube in the path of detection, the fluorescence signal was divided into two polarization channels – one parallel and one perpendicular to the direction of polarization of the excitation source. The background signal measured from tetraborate buffer in the ECI illuminated by a polarized light source was divided 2 : 1 between parallel and perpendicular channels. The start–stop time (lifetime) histogram features a sharp peak indicating that a considerable amount of Raman scattering contributed to the background (Fig. 5a). Therefore, software gating was employed to suppress this background by excluding photons arriving within a short window following the excitation pulse.

Fig. 5b shows the *S*/*N* ratio as a function of the width of the off-gate applied to the lifetime histogram of 10 s wide peak in the electropherogram of a plug of 100 pM fluorescein. The *S*/*N* is calculated from the amplitude of the peak of the plug (*S*) and the standard deviation of the intensity trajectory before the plug arrival (*N*). Note that even in the absence of lifetime gating, the *S*/*N* in the perpendicular channel is higher than that in the parallel channel by *ca.* 60%. The optimum time gating window (0.4 ns) improved the *S*/*N* mainly in the perpendicular channel (40%) and to a smaller extent in the sum of two channels (30%). However, in our setup, the highest absolute value of the *S*/*N* was

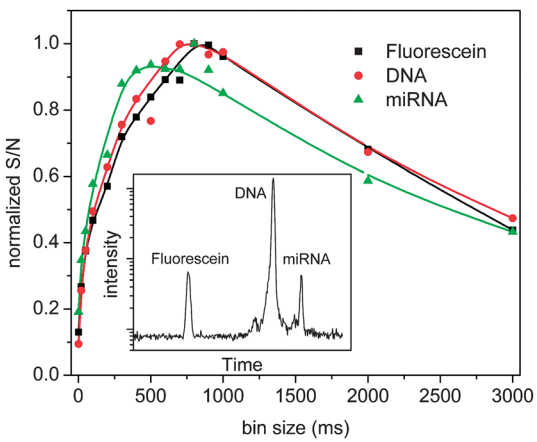

Fig. 4 Normalized *S*/*N* data *versus* data binning time for electrophoretic separation of fluorescein (100 pM), DNA probe (5 nM) and DNA–miRNA hybrid (100 pM).

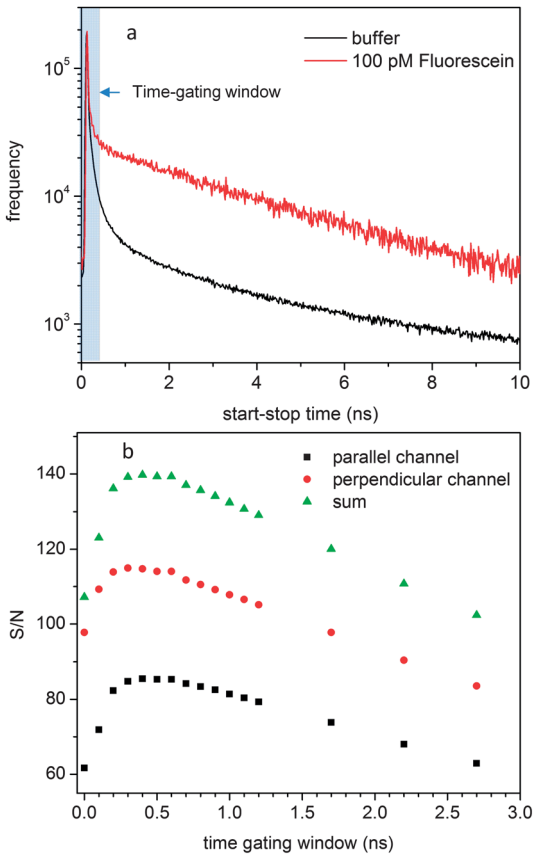

Fig. 5 (a) Lifetime histogram of tetraborate buffer (black) and 100 pM fluorescein (red) measured inside the ECI. (b) *S*/*N* ratio of 100 pM fluorescein as a function of time gating window.

observed for the sum of two polarization channels (green curve, Fig. 5b). All subsequent measurements were performed with all photons falling on a single SPAD, by using 0.4 ns gating window and no polarization filtering. Time-resolved detection can provide further improvement in *S*/*N* if fluorescent labels with longer lifetimes (>5 ns) are used in combination with fast detectors (response time < 100 ps). In addition, more sophisticated lifetime filtering in software can be used to distinguish different fluorescence species from one another, even when their emission peaks overlap.[36]

3.4. Detection sensitivity (mLOD, cLOD, MCE and LOD)

To characterize the sensitivity of our CE-CMPF-ECI setup, 60 pL of samples of serially diluted fluorescein were injected into the capillary and propagated to the detector using electrophoresis. Samples containing roughly 3200, 1600, 800, 400 and 200 molecules were studied. The resulting *S*/*N* values of the fluorescein peaks, plotted as a function of the number of injected molecules, follow a linear trend ($R^2 = 0.998$) and give a $S/N = 3$ at 50 molecules (mLOD) (Fig. 6). This value is a theoretical limit, which is calculated by assuming a linear dependence of the signal detected on the number of molecules injected, which may not be valid as the number of molecules becomes smaller. However, as seen in Fig. 6A, for the most diluted sample, which contains only 200 molecules, the signal is well above the fluctuations of the background and the calculated limit of detection of 50 molecules

seems very plausible. The concentration of this sample was 1.5 pM, giving a cLOD comparable to those achieved using burst analysis in tight capillaries (250 fM (ref. 17) and 2 pM (ref. 22)). The error bars indicated in Fig. 6 represent a 15% variation and were determined by measuring the variation in peak area between 10 separate 60 pL injections of 100 pM fluorescein. This error is presumably due to some irreproducibility in the volume of sample injected by the automated syringe pump.

To determine the MCE and LOD of our setup we estimated the fraction of injected molecules passing through the detection volume by dividing the cross-section of the detection volume, as measured perpendicular to the capillary's axis, by the cross-section of the capillary's inner bore. Based on the results of the FCS measurements an MCE of ~13% was estimated, which, combined with the mLOD value of 50, yields a LOD of 6.5 molecules of fluorescein for our instrument. This LOD is comparable to results achieved using off-column designs and the mLOD is 3 orders of magnitude better than those achieved using a commercial CE instrument.

3.5. Application to biological samples

In addition to creating a sensitive on-column CE-LIF instrument, our goal was also to design a setup that could analyze crude biological samples such as cell lysate and that could directly perform commercial CE protocols. As a proof-of-principle of the latter two goals we used CE-CMPF-ECI to perform the DQAMmiR protocol previously developed on a commercial instrument.[28] DQAMmiR is used to directly detect native miRNA species from cell lysate samples. Using fluorescently labeled ssDNA probes designed as complements to specific miRNA species, the probe–miRNA hybrids are separated from the unbound probes using CE and the miRNA content is quantified. The method is applicable to multiple miRNA species by using different probes with different drag tags, which shift the probe migration times from one another. Also the run buffer contains excess of SSB, which shifts the migration times of all unbound probes from those that are bound.

Samples containing three DNA probes mixed with known, and equal, concentrations of three miRNA species were analyzed using CE-CMPF-ECI and the commercial CE instrument. The results are shown in Fig. 7 and demonstrate similar *S*/*N* ratios for similar peaks, despite the fact that the CE-CMPF-ECI samples contained 600-times fewer miRNAs. Also notable was the fact that baseline separation was achieved by CE-CMPF-ECI in one-third of the separation time required by the commercial CE instrument. By extrapolating the average *S*/*N* ratios of the three hybrid peaks down to $S/N = 3$, the miRNA mLOD of each setup can be determined. This gives the values of 10^5 and 200 miRNA copies for commercial CE and CE-CMPF-ECI instruments, respectively, *i.e.*, a 500× improvement in sensitivity on our setup. In addition, this number is better compared to the number we reported previously (300×)[37] due to the application of optimized time binning in this work (600 ms *vs.* 100 ms, see above).

To show that our setup was also effective for the analysis of complex biological samples, we performed the DQAMmiR protocol on a sample of MCF-7 cell lysate. Though the use of cell lysate changes the conductivity of the sample and affects the migration times of analytes (with respect to Fig. 7), the use of an internal standard allows the time axis to be scaled for inter-run comparisons. Fig. 8 shows the data from similar samples measured on the CE-CMPF-ECI setup and the commercial CE instrument. The two electropherograms are identical except for some fine-structure detail on the SSB-DNA probe peak and the internal standard peak, and a significant difference in the miRNA–DNA peak height. The first two discrepancies are understood to be due to the high sensitivity of the CE-CMPF-ECI, which picks up small details that may have otherwise gone unnoticed. The difference in the miRNA–DNA hybrid peak height is because 1200-times more lysate was used for the commercial CE than for the CE-CMPF-ECI.

The small injection volumes required for analysis by CE-CMPF-ECI also allow for the possibility of analyzing the contents of a single cell. In order to test this capability, we injected the amount of cell lysate equivalent to that of a single cell and analyzed it using the DQAMmiR probes.[37] We were able to detect a peak of the DNA–mir21 hybrid with an area that corresponded to roughly 12 000 copies of mir21 per cell. This number agrees with measurements made using other methods[38]

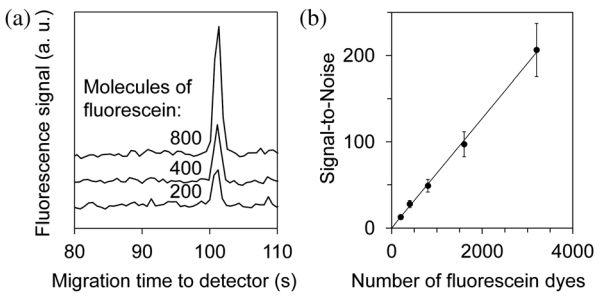

Fig. 6 Left: stacked electropherograms showing the peak size of 60 pL injections of fluorescein of different concentrations: 25 pM, 12 pM, and 6 pM, respectively. Right: the *S*/*N* ratio of the electropherograms was used to determine a linear calibration curve which indicates a $S/N = 3$ for ~50 molecules of fluorescein.

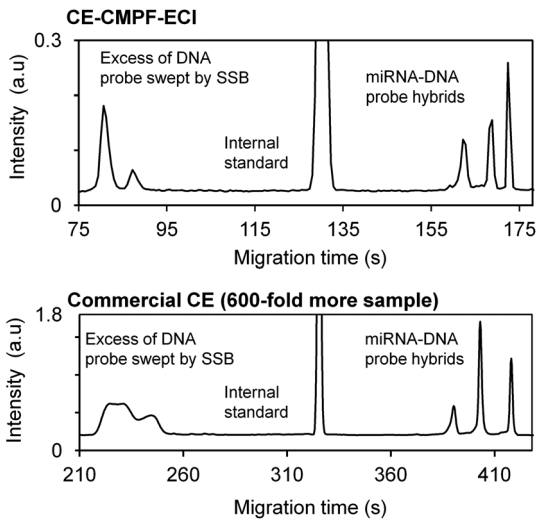

Fig. 7 Three miRNA species (from left to right, mir145, mir125b, mir21) spiked into a sample containing an internal standard (IS) and a 5-fold excess of probes. The sample is injected and separated by CE in a running buffer containing SSB. Electopherograms for CE-CMPF-ECI (top) and a commercial CE instrument (bottom) are shown.

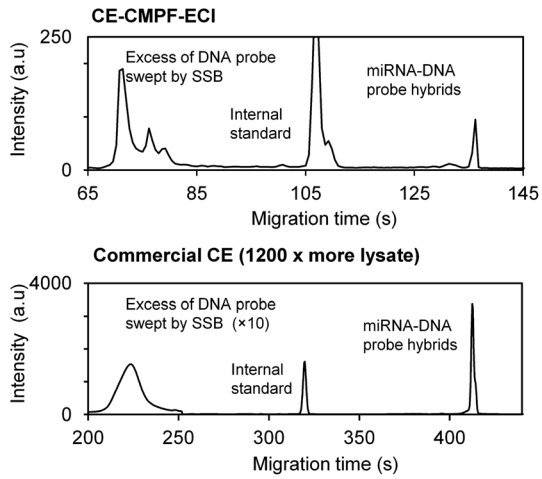

Fig. 8 Three DNA probes are incubated in a sample of MCF-7 cell lysate along with an internal standard. The sample is injected and separated by CE in a running buffer containing SSB. Results obtained with CE-CMPF-ECI (top) and a commercial CE instrument (bottom) are shown. Only one miRNA species is detectable (mir21) using both instruments. Around 1200× more cell lysate (and hence miRNA) was injected in the lower trace.

and thus opens up interesting possibilities of using the CE-CMPF-ECI approach for single cell analytics.

4. Conclusions

In this study, we described the development and characterization of ultrasensitive capillary electrophoresis on a confocal setup. An embedded capillary interface was designed using a commercially available capillary and a simple protocol. This interface allowed highly sensitive measurements to be carried out in capillary using multiparameter fluorescence detection on a confocal microscope. The signal-to-noise ratio was investigated by optimizing the excitation power, signal binning time, lifetime and polarization filtering after data acquisition. Sensitive CE experiments were carried out using this setup and a limit of detection of 6.5 fluorescein molecules was achieved, comparable to those achieved by off-column and custom capillary designs. By performing on-column detection in a commercially available capillary we showed our design to be able to robustly perform: (i) methods previously developed on commercial instruments, and (ii) the analysis of samples of cell lysate down to the contents of a single cell. In addition, our design was constructed entirely from commercially available parts making it accessible to a wide research community.

Acknowledgements

A.M. and B.J.D. contributed equally to this manuscript. The work was funded by the Natural Sciences and Engineering Research Council of Canada.

References

1 R. J. Meagher, J. I. Won, L. C. McCormick, S. Nedelcu, M. M. Bertrand, J. L. Bertram, G. Drouin, A. E. Barron and G. W. Slater, *Electrophoresis*, 2005, **26**, 331–350.
2 M. C. Ruizmartinez, J. Berka, A. Belenkii, F. Foret, A. W. Miller and B. L. Karger, *Anal. Chem.*, 1993, **65**, 2851–2858.
3 F. Wan, W. D. He, J. Zhang and B. Chu, *Electrophoresis*, 2009, **30**, 2488–2498.
4 C. I. D. Newman and G. E. CollinS, *Electrophoresis*, 2008, **29**, 44–55.
5 M. Berezovski and S. N. Krylov, *J. Am. Chem. Soc.*, 2002, **124**, 13674–13675.
6 S. N. Krylov, *Electrophoresis*, 2007, **28**, 69–88.
7 X. J. Liu, F. Dahdouh, M. Salgado and F. A. Gomez, *J. Pharm. Sci.*, 2009, **98**, 394–410.
8 Y. H. Chu, L. Z. Avila, H. A. Biebuyck and G. M. Whitesides, *J. Med. Chem.*, 1992, **35**, 2915–2917.
9 N. H. H. Heegaard and F. A. Robey, *Anal. Chem.*, 1992, **64**, 2479–2482.
10 S. M. Wang, L. Fan and S. Y. Cui, *J. Sep. Sci.*, 2009, **32**, 3184–3190.
11 F. Kitagawa and K. Otsuka, *J. Chromatogr., B: Anal. Technol. Biomed. Life Sci.*, 2011, **879**, 3078–3095.
12 N. J. Dovichi, J. C. Martin, J. H. Jett, M. Trkula and R. A. Keller, *Anal. Chem.*, 1984, **56**, 348–354.
13 Y. F. Cheng and N. J. Dovichi, *Science*, 1988, **242**, 562–564.
14 D. Y. Chen, K. Adelhelm, X. L. Cheng and N. J. Dovichi, *Analyst*, 1994, **119**, 349–352.
15 D. Y. Chen and N. J. Dovichi, *J. Chromatogr., B: Biomed. Sci. Appl.*, 1994, **657**, 265–269.
16 O. O. Dada, D. C. Essaka, O. Hindsgaul, M. M. Palcic, J. Prendergast, R. L. Schnaar and N. J. Dovichi, *Anal. Chem.*, 2011, **83**, 2748–2753.
17 A. Lundqvist, D. T. Chiu and O. Orwar, *Electrophoresis*, 2003, **24**, 1737–1744.
18 M. Foquet, J. Korlach, W. R. Zipfel, W. W. Webb and H. G. Craighead, *Anal. Chem.*, 2004, **76**, 1618–1626.
19 B. Huang, H. K. Wu, D. Bhaya, A. Grossman, S. Granier, B. K. Kobilka and R. N. Zare, *Science*, 2007, **315**, 81–84.
20 B. J. Xu, M. Yang, H. Wang, H. L. Zhang, Q. H. Jin, J. L. Zhao and H. M. Wang, *Sens. Actuators, A*, 2009, **152**, 168–175.
21 P. G. Schiro, C. L. Kuyper and D. T. Chiu, *Electrophoresis*, 2007, **28**, 2430–2438.
22 B. B. Haab and R. A. Mathies, *Anal. Chem.*, 1999, **71**, 5137–5145.
23 K. Dorre, J. Stephan and M. Eigen, *Single Mol.*, 2001, **2**, 165–175.
24 C. Zander, K. H. Drexhage, K. T. Han, J. Wolfrum and M. Sauer, *Chem. Phys. Lett.*, 1998, **286**, 457–465.
25 D. K. Lloyd and H. Watzig, *J. Chromatogr., B: Biomed. Sci. Appl.*, 1995, **663**, 400–405.
26 I. Miksik and Z. Deyl, *J. Chromatogr., A*, 1999, **852**, 325–336.
27 S. Pennathur and J. G. Santiago, *Anal. Chem.*, 2005, **77**, 6772–6781.
28 D. W. Wegman and S. N. Krylov, *Angew. Chem., Int. Ed.*, 2011, **50**, 10335–10339.
29 D. Cohen, J. A. Dickerson, C. D. Whitmore, E. H. Turner, M. M. Palcic, O. Hindsgaul and N. J. Dovichi, *Annu. Rev. Anal. Chem.*, 2008, **1**, 165–190.
30 B. Liu, S. Fletcher, M. Avadisian, P. T. Gunning and C. C. Gradinaru, *J. Fluoresc.*, 2009, **19**, 915–920.
31 A. Mazouchi, B. Liu, A. Bahram and C. C. Gradinaru, *Anal. Chim. Acta*, 2011, **688**, 61–69.
32 B. B. Haab and R. A. Mathies, *Anal. Chem.*, 1995, **67**, 3253–3260.
33 A. Castro and E. B. Shera, *Anal. Chem.*, 1995, **67**, 3181–3186.
34 J. Enderlein, *Opt. Commun.*, 1999, **160**, 201–206.
35 M. Kanoatov and S. N. Krylov, *Anal. Chem.*, 2011, **83**, 8041–8045.
36 H. He, B. K. Nunnally, L. C. Li and L. B. McGown, *Anal. Chem.*, 1998, **70**, 3413–3418.
37 B. J. Dodgson, A. Mazouchi, D. W. Wegman, C. C. Gradinaru and S. N. Krylov, *Anal. Chem.*, 2012, **84**, 5470–5474.
38 H. M. Chan, L. S. Chan, R. N. S. Wong and H. W. Li, *Anal. Chem.*, 2010, **82**, 6911–6918.